Depleting MET-expressing tumor cells by ADCC provides a therapeutic advantage over inhibiting HGF/MET signaling

Research Article

Depleting MET-expressing tumor cells by ADCC provides a therapeutic advantage over inhibiting HGF/MET signaling

Anna Hultberg[1]*, Virginia Morello[2,3]*, Leander Huyghe[4], Natalie De Jonge[1], Christophe Blanchetot[1], Valérie Hanssens[1], Gitte de Boeck[1], Karen Silence[1], Els Festjens[1], Raimond Heukers[5], Benjamin Roux[6], Fabienne Lamballe[6], Christophe Ginestier[7], Emmanuelle Charafe-Jauffret[7], Flavio Maina[6], Peter Brouckaert[4], Michael Saunders[1], Alain Thibault[1], Torsten Dreier[1], Hans de Haard[1], and Paolo Michieli[2,3]

[1]arGEN-X BVBA, Zwijnaarde, Belgium; [2]Department of Oncology, University of Torino Medical School, Candiolo, Turin, Italy; [3]Laboratory of Experimental Therapy, Candiolo Cancer Institute - FPO, IRCCS, Candiolo, Turin, Italy; [4]Department of Molecular Biomedical Research, Inflammation Research Center, Ghent University, Zwijnaarde, Belgium; [5]Department of Biology, Utrecht University, Utrecht, The Netherlands; [6]Aix-Marseille Université, IBDM, CNRS UMR 7288, Parc Scientifique de Luminy, Marseille, France; [7]Aix-Marseille Université, CRCM, Institut Paoli-Calmettes, CNRS UMR 7258, Marseille, France.

*These authors contributed equally to this work.

Address correspondence to: A.H. for antibody-related matters (ahultberg@argen-x.com) and P.M. for HGF/MET biology (paolo.michieli@ircc.it).

Running title: *ARGX-111 kills MET-expressing cancer cells by ADCC*

Keywords: *HGF, ADCC, targeted therapy, circulating tumor cells, metastasis*

Correspondence with Editorial and Production offices: P.M. (paolo.michieli@ircc.it).

Full address of corresponding authors:

Anna Hultberg, arGEN-X BVBA, Technologiepark 30, arGEN-X BVBA, B-9052 Zwijnaarde, Belgium. Phone: +32-9-2434077.

Paolo Michieli, Laboratory of Experimental Therapy, Candiolo Cancer Institute – FPO, IRCCS, SP 142 km 3.95, I-10060 Candiolo, Turin, Italy. Phone: +39-011-9933219.

Grant support: This work was supported by IWT (Agentschap voor Innovatie door Wetenschap en Technologie) grants # IWT090297 and IWT100440, by Italian Association for Cancer Research (AIRC 2010 Special Program in Molecular Clinical Oncology 5‰ Project n. 9970 and AIRC 2012 IG grant n. 12798), and the University of Torino/Compagnia di San Paolo (Progetti di Ricerca di Ateneo 2012).

Financial disclosure: A.H., N.D.J., C.B., V.H., G.d.B., K.S., M.S., A.T., T.D. and H.d.H. are all employees of arGEN-X. E.F. is a former employee of arGEN-X. P.M. is a consultant for arGEN-X. The other authors declare no conflict of interest.

Manuscript information: 5,857 words (excluding references), 7 figures, 7 supplementary figures, 7 supplementary tables, supplementary methods.

ABSTRACT

Hepatocyte growth factor (HGF) and its receptor MET represent validated targets for cancer therapy. However, HGF/MET inhibitors being explored as cancer therapeutics exhibit cytostatic activity rather than cytotoxic activity, which would be more desired. In this study, we engineered an antagonistic anti-MET antibody that, in addition to blocking HGF/MET signaling, also kills MET-overexpressing cancer cells by antibody-dependent cellular cytotoxicity (ADCC). As a control reagent, we engineered the same antibody in an ADCC-inactive form that is similarly capable of blocking HGF/MET activity, but in the absence of any effector function. In comparing these two antibodies in multiple mouse models of cancer, including HGF-dependent and -independent tumor xenografts, we determined that the ADCC-enhanced antibody was more efficacious than the ADCC-inactive antibody. In orthotopic mammary carcinoma models, ADCC enhancement was crucial to deplete circulating tumor cells and to suppress metastases. Prompted by these results, we optimized the ADCC-enhanced molecule for clinical development generating an antibody (ARGX-111) with improved pharmacological properties. ARGX-111 competed with HGF for MET binding, inhibiting ligand-dependent MET activity; down-regulated cell surface expression of MET, curbing HGF-independent MET activity; and engaged NK cells to kill MET-expressing cancer cells, displaying MET-specific cytotoxic activity. ADCC assays confirmed the cytotoxic effects of ARGX-111 in multiple human cancer cell lines and patient-derived primary tumor specimens, including MET-expressing cancer stem-like cells. Together, our results show how ADCC provides a therapeutic advantage over conventional HGF/MET signaling blockade, and generate proof-of-concept for ARGX-111 clinical testing in MET-positive oncological malignancies.

INTRODUCTION

MET, the product of the c-*MET* proto-oncogene, is a transmembrane tyrosine kinase that is expressed by the majority of epithelial tissues and by endothelial, muscle, neuronal, hematopoietic and immune cells (1). The high affinity ligand of MET, hepatocyte growth factor (HGF), is a pleiotropic cytokine that is secreted by cells of mesenchymal origin, typically fibroblasts and macrophages (2). HGF signaling through MET promotes a peculiar biological program that results from the fine orchestration of complementary biological activities including pro-migratory, mitogenic and anti-apoptotic cues (3). This process, known collectively as invasive growth, is essential for embryogenesis, during which HGF/MET signaling is responsible for migration, proliferation and survival of various progenitor cells (4). In normal adult tissues, HGF-driven invasive growth is usually quiescent, but is resumed following tissue injury to promote wound healing and tissue regeneration (5).

While HGF/MET signaling is tightly controlled in normal tissues, it is frequently subverted in tumors, which exploit the invasive growth program in order to grow within and to colonize the host organism (6). HGF overexpression in the tumor microenvironment correlates with increased tumor aggressiveness and invasion (7). HGF is also a powerful pro-angiogenic factor promoting tumor angiogenesis (8). Aberrant activation of MET is frequently observed in human cancer and can be due to different molecular mechanisms, including c-*MET* transcriptional activation, amplification or mutation, as well as autocrine or paracrine HGF stimulation (9). In the clinic, MET protein overexpression and c-*MET* gene amplification have been identified as negative prognostic markers for a variety of oncological diseases, including lung (10), colon (11), breast (12), head and neck (13) and gastric (14) carcinoma, as well as multiple myeloma (15) and glioblastoma multiforme (16).

Several inhibitors have been developed so far to tackle HGF/MET activity in cancer, including small

molecule MET tyrosine kinase inhibitors, anti-HGF antibodies and anti-MET antibodies (17-19). Surprisingly, and in striking contrast to the importance of HGF/MET signaling for survival of different cell types during embryogenesis, HGF- or MET-targeted drugs have however demonstrated cytostatic rather than cytotoxic activity on tumor cells, independently of their mechanism of action (20, 21). In fact, even in the most MET-dependent tumors displaying c-*MET* gene amplification, inhibition of MET activity leads to G1 arrest and not to cell death, both in cellular studies and in xenografts (22). Consistent with this idea, HGF/MET signaling in cancer cells is typically associated with promotion of epithelial-to-mesenchymal transition (EMT) and with tumor progression rather than with tumor onset (1, 4, 6, 9).

To overcome this pharmacological limitation, and to investigate whether MET-targeted cytotoxicity would confer a therapeutic advantage over plain HGF/MET inhibition, we engineered an antagonistic anti-MET antibody that, in addition to blocking both HGF-dependent and -independent MET activation, displays enhanced antibody-dependent cellular cytotoxicity (ADCC). At the same time, we also engineered an ADCC-dead version of the same antibody that inhibits HGF/MET signaling but is completely devoid of any effector function, and compared the anti-tumor and anti-metastasis activity of this antibody pair in multiple mouse models of cancer. The results presented here suggest that killing MET-expressing cancer cells by ADCC is significantly more effective from a therapeutic viewpoint than simply inhibiting HGF/MET signaling.

MATERIALS AND METHODS

Cell culture

A549, BxPC3, MDA-MB-231, NCI-H1437, NCI-H2122, NCI-H441, NCI-H596, Raji, SNU-5, TOV-112D, U87-MG and 786-O cells were purchased from the American tissue Type Culture Collection (ATCC). A498, L540, MKN-45 and U266 cells were purchased from the Deutsche Sammlung von Mikroorganismen und Zellkulturen (DSMZ). EBC-1 cells were purchased from the Japanese Collection of Research Bioresources (JCRB). All cells were cultured according to the protocols provided by the supplier and used within 6 months after receipt or validated by short tandem repeat profiling using Cell ID™ System (Promega). LOC cells (23), immortalized human mammary fibroblasts (24) and CRCM tumors (25) have been described previously.

ADCC assays

ADCC of MKN-45, NCI-H441 and A549 cells was determined with a standard ^{51}Cr release assay (26) using human peripheral blood mononuclear cells from 3 different donors (Etablissement Français Du Sang) and a 50:1 effector:target ratio. All experiments were performed in triplicate. Percent lysis was analyzed versus antibody concentration, and the EC_{50} and E_{MAX} values were calculated using Prism software (GraphPad). ADCC of MDA-MB-231 cells and of primary triple negative mammary carcinoma cells was analyzed using an ADCC Reporter Bioassay Kit (Promega). Single cell suspensions were stained with AldeFluor™ (Stemcell Technologies) and then sorted by FACS using a MoFlo™ XDP cell sorter (Beckman Coulter). ALDH-1$^+$ cells were incubated with increasing ARGX-111 concentrations (0-667 nM) and reporter effector cells (effector:target ratio 2.5:1), and ADCC was measured as described by the manufacturer. Data were analyzed and fit using Prism software (GraphPad).

Subcutaneous xenograft mouse models

U87-MG or MKN-45 cells (3×10^6 cells/mouse) were injected s.c. into the right or left hind flank of 6-8 week-old CD-1 nude mice (Charles River). When tumor volume approached 100 mm^3, mice were randomly assigned to 3 treatment arms (U87-MG, 10 mice/group; MKN-45, 6 mice/group): irrelevant IgG1; WT52-E; and WT52-D. Antibodies were administered two times a week by i.p. injection, and tumor volume was monitored over time as described (24). At autopsy, tumor weight was determined on freshly explanted tumors (U87-MG). For analysis of MET and phospho-MET levels, mice bearing MKN-45 tumors were treated with a single bolus of WT52-E or irrelevant IgG1 (3 mice/group) and tumors were extracted for analysis 24 hours later. Tumor sections were analyzed by immuno-histochemistry using anti-MET or anti-phospho-MET antibodies (both from LSBio).

Orthotopic mammary carcinoma models

For the neo-adjuvant setting, MDA-MB-231-luc cells were mixed 4:1 with immortalized human mammary fibroblasts and then injected bilaterally (2.5×10^6 cells/injection site) into the mammary fat pad of 6 week-old female CB17 SCID mice (Charles River) as described (24). After 3 weeks, mice were stratified based on tumor volume and randomly assigned to the following treatment arms (n = 8): IgG1; WT52-E; WT52-D. Antibodies were administered 2 times a week by i.p. injection at a dose of 5 mg/kg IgG1. Tumor growth was monitored over time as described (24). After 4 weeks of treatment, tumors were surgically removed, and neo-adjuvant therapy was interrupted. Two weeks after surgery, mice were injected with luciferin, sacrificed, and subjected to autopsy. Metastatic dissemination was determined by bioluminescence analysis of isolated lungs and femurs as described (24). The number of CTCs was determined at the indicated time points by measuring luciferase activity on mouse blood. Approximately 100 µl of whole blood was cleared from erythrocytes using red blood cell lysis buffer (BD Biosciences), and CTCs were collected by centrifugation. The cell pellet was washed in PBS and then

lysed in 20 µl luciferase assay buffer (Promega). Luciferase activity was measured on 10 µl of cell lysate using a Luciferase Reporter Assay System kit (Promega). Samples were analyzed with a GloMax 96 Microplate Luminometer (Promega). Estimation of CTC number was calculating using a standard curve of luciferase-expressing MDA-MB-231 cells. For the adjuvant setting, MDA-MB-231-luc cells were injected orthotopically into the mammary fat pad of 6 week-old female CB17 SCID mice along with human mammary fibroblasts as described above, and CTCs were determined at regular time intervals. Primary tumors were removed by surgery approximately 5 weeks after cell injection. Two days after surgery, mice were randomized based on CTC number and assigned to 3 treatment arms (10 mice/group) as above (IgG1, WT52-E, WT52-D; 5 mg/kg). After 4 weeks of treatment, mice were sacrificed and metastatic dissemination was assessed by bioluminescence analysis of whole body and isolated organs as described (24).

Study approval

All procedures involving the use of animals and/or human samples were authorized by the competent authorities. Please see online supplementary methods for more information.

Supplementary online material

The supplementary online material section comprises supplementary figures 1-7, supplementary tables 1-7 and supplementary methods.

RESULTS

Generation of an ADCC-enhanced antagonistic anti-MET antibody for mouse studies

We recently reported the generation of a wide panel of chimeric llama-human antagonistic anti-MET antibodies (24). The most antagonistic molecule within this panel (WT52) blocks both HGF-dependent MET activity (by competing with HGF for binding to MET; Suppl. Fig. S1A-B) and HGF-independent MET activity (by promoting MET internalization; Suppl. Fig. S1C-D). WT52 was engineered to an ADCC-enhanced version (WT52-E) by introducing the S239D/I332E amino acid substitutions in the CH2 domain (27). As a control, an ADCC-inactive ('dead') mutant version of WT52 (WT52-D) was also engineered that contained the E233P/L234V/L235A amino acid substitutions in the CH2 domain (26). ELISA analysis of Fc receptor binding revealed that WT52-E displays increased affinity for human FcγRIIIa and its mouse orthologue FcγRIV, as well as for human and mouse FcγRI compared to WT52 (Suppl. Tab. S1). WT52-D displayed very low affinity for human FcγRI and no affinity for human FcγRIIIa, mouse FcγRI or mouse FcγRIV. In in vitro ADCC assays using effector cells from 3 distinct donors, WT52-E displayed a tumor cell killing activity directly proportional to MET expression levels and invariably superior to that of WT52 (Suppl. Tab. S2). WT52-D did not display any ADCC activity in any cell line tested.

ADCC enhancement results in improved anti-tumor activity in both HGF-dependent and -independent xenograft models

In order to determine whether ADCC enhancement provides an advantage over plain HGF/MET inhibition in mouse models of cancer, we tested the WT52-E/WT52-D antibody pair in both HGF-dependent and -independent xenograft systems. U87-MG cells, which display an autocrine HGF/MET loop (28), were injected subcutaneously into CD-1 nude mice (that have functional NK cells and are

therefore ADCC-competent) to induce the formation of experimental tumors. Tumor-bearing mice were randomly assigned to 3 treatment arms (irrelevant IgG1; WT52-E; WT52-D), and antibodies were administered at a dose of 5 mg/kg. Tumor burden analysis revealed that WT52-E and WT52-D inhibited tumor growth by 88% (p = 0.0003) and 51% (p = 0.0159), respectively (Fig. 1A). At the end of the experiment, the mean weight of control tumors was 1819 ± 331 mg, while that of antibody-treated tumors was 295 ± 103 mg (WT52-E) and 930 ± 215 mg (WT52-D; Fig. 1B). The activity of WT52-E and WT52-D was also tested in a HGF-independent mouse model of cancer. MKN-45 human gastric carcinoma cells, which display constitutive, ligand-independent MET activation (29), were injected subcutaneously into CD-1 nude mice. Tumor-bearing mice were randomized into 3 treatment arms as above (IgG1; WT52-E; WT52-D), and antibodies were administered at a dose of 1 mg/kg. In this model, WT52-E and WT52-D inhibited tumor growth by 85% (p = 0.0018) and 54% (p = 0.0355), respectively (Fig. 1C). In a separate experiment using CD-1 nude mice bearing MKN-45 tumors, a single bolus of WT52-E (5 mg/kg) resulted in a significant reduction of both phospho-MET and total MET levels (Fig. 1D). Taken together, these results suggest that ADCC enhancement provides a therapeutic advantage over plain HGF/MET signaling inhibition in both HGF-dependent and -independent xenograft models.

MET-targeted ADCC inhibits tumor growth and metastasis in a neo-adjuvant orthotopic mammary carcinoma model

We recently reported that anti-MET antagonistic antibodies inhibit tumor growth and suppress metastatic dissemination in an orthotopic model of mammary carcinoma (24). In order to explore the therapeutic potential of MET-targeted ADCC in this model, we injected MDA-MB-231 human triple-negative mammary carcinoma cells expressing luciferase (MDA-MB-231-luc) into the mammary fat pad of SCID mice (which have functional NK cells and are therefore ADCC-competent). Since mouse HGF does not activate human MET, tumor cells were injected along with HGF-secreting, immortalized human

mammary fibroblasts (24). Tumor-bearing mice were randomly assigned to 3 treatment arms as above (IgG1; WT52-E; WT52-D), and antibodies were administered at a dose of 5 mg/kg. After 4 weeks of treatment, tumors were surgically removed, and neo-adjuvant therapy was interrupted. Two weeks after surgery, mice were injected with luciferin, sacrificed, and subjected to autopsy. Metastatic dissemination was determined by bioluminescence analysis of isolated lungs and femurs (Fig. 2A). This analysis revealed that WT52-E and WT52-D reduced tumor growth by 57% ($p < 0.0001$) and 20% ($p = 0.0271$), respectively (Fig. 2B). Interestingly, however, the effect of anti-MET antibodies was greater on metastases. In fact, WT52-E and WT52-D reduced lung metastases (Fig. 2C) by 91% ($p = 0.0090$) and 74% ($p = 0.0294$), respectively, and femur metastases (Fig. 2D) by 95% ($p = 0.0047$) and 79% ($p = 0.0158$). We also monitored the number of circulating tumor cells (CTCs) during the whole experiment by measuring luciferase activity in the blood. Before surgery, we observed neither a correlation between CTC number and tumor volume nor a significant difference in CTC number among the various experimental groups (Fig. 2E). However, interestingly, once the primary tumors were removed, mice treated with WT52-E displayed significantly reduced CTC number and metastases compared to both the WT52-D and the control group (Fig. 2F).

Adjuvant MET-targeted ADCC suppresses metastasis by eliminating circulating tumor cells

Metastasis onset following tumor resection is typically due to the seeding of CTCs at secondary anatomical sites. Unfortunately, surgery itself is often a cause of tumor cell spreading. Prompted by this consideration, we explored the therapeutic potential of MET-targeted ADCC in an adjuvant model of metastatic mammary carcinoma in which treatment started after tumor resection. MDA-MB-231-luc cells and HGF-secreting human fibroblasts were injected orthotopically into the mammary fat pad of SCID mice as described above, and CTCs were determined at regular time intervals. Primary tumors were removed by surgery approximately 5 weeks after cell injection. Two days after surgery, mice were

randomized based on CTC number and assigned to 3 treatment arms as above (IgG1; WT52-E; WT52-D; 5 mg/kg). After 4 weeks of treatment, mice were sacrificed and metastatic dissemination was assessed by bioluminescence analysis of whole body and isolated organs (Fig. 3A). Consistent with our work hypothesis, CTC number burst soon after surgery and then returned to lower levels in approximately a week (Fig. 3B). However, while CTC number in mice receiving WT52-E remained low over time, it tended to climb up again in mice treated with control IgG1 or with WT52-D. At sacrifice, the WT52-E group displayed 89% less CTCs compared to the IgG1 arm (p = 0.0274) and 81% less CTCs compared to the WT52-D arm (p = 0.0383; Fig. 3C). In vivo imaging (Suppl. Fig. S2) revealed that WT52-E dramatically reduced whole body bioluminescence compared to both IgG1 (86%, p = 0.0035) and WT52-D (81%, p = 0.0397; Fig. 3D). Bioluminescence analysis of explanted lungs unveiled that WT52-E potently suppressed pulmonary metastases compared to both IgG1 (93%, p = 0.0361) and WT52-D (91%, p = 0.0499; Fig. 3E). Similarly, WT52-E-treated mice displayed reduced bone metastases compared to both control mice (88%, p = 0.0277) and mice of the WT52-D arm (82%, p = 0.0446; Fig. 3F). Interestingly, CTC number in each mouse showed a direct correspondence with metastatic dissemination (Suppl. Fig. S3). We conclude that killing CTCs by MET-targeted ADCC may be an effective strategy to prevent tumor recurrence and to suppress metastatic dissemination.

Generation of ARGX-111, an ADCC-enhanced anti-MET antibody for clinical development

The results obtained in mouse models of cancer suggest that MET-targeted ADCC achieves superior tumor inhibition and metastasis suppression compared to HGF/MET signaling blockade. Prompted by these data, we set to develop an ADCC-enhanced anti-MET antibody for clinical use. The llama WT52 VH and VL framework regions display 88% average human identity. Using phage display-based affinity enrichment, we selected a molecule with 95% human framework identity (G52; Suppl. Fig. S4). Germlining did not affect the major biochemical and biological characteristics of the antibody (Suppl.

Tab. S3). G52 was further optimized by introducing the H433K/N434F substitutions in the CH3 region, generating the G52-HN antibody. These substitutions are known to increase binding to human FcRn at acidic pH while not affecting its affinity at neutral pH, thus enhancing antibody recycling from the sorting endosome (30). Surface Plasmon Resonance confirmed that G52-HN has a K_D for human FcRn at pH 6.0 that is approximately 6 times lower compared to G52 (0.255 ± 0.01 nM vs. 1.37 ± 0.11 nM). G52-HN was produced in a GS-CHO cell line lacking alpha-1,6-fucosyltransferase, thus obtaining an afucosylated G52-HN antibody (hereafter referred to as ARGX-111). Antibody afucosylation is known to increase affinity for human FcγRIIIa, thus resulting in enhanced ADCC (31). ELISA analysis confirmed that afucosylation increased antibody binding to both V158 FcγRIIIa and F158 FcγRIIIa by at least 25 times, while it did not significantly affect hFcγRI binding (Suppl. Tab. S4). The major biochemical and pharmacological characteristics of ARGX-111 are summarized in Suppl. Fig. S5.

ARGX-111 inhibits HGF-dependent MET activity by competing with HGF for binding to MET

The ability of ARGX-111 to inhibit HGF-dependent MET activity was determined in a variety of biochemical and biological assays. Flow cytometry analysis on a panel of human tumor cell lines expressing different MET levels unveiled that ARGX-111 binds to native MET with an EC_{50} ranging from 0.1 nM to 0.7 nM (Suppl. Tab. S5). In ELISA assays, ARGX-111 competed with HGF displaying an IC_{50} of 1.3 nM and an I_{MAX} of 95% (Fig. 4A). In MET activation experiments using A549 cells, ARGX-111 inhibited HGF-induced MET auto-phosphorylation with an IC_{50} of 5.3 nM and an I_{MAX} of 74% (Fig. 4B). Similar results were obtained using NCI-H1437 NSCLC cells (IC_{50} = 13.2 nM; I_{MAX} = 60%; Fig. 4C). In a HGF-dependent cell migration assay using A549 cells seeded in a Boyden chamber, ARGX-111 completely neutralized the pro-migratory effect of HGF (Fig. 4D). In an anchorage-independent growth assay using NCI-H1437 cells seeded in soft agar, ARGX-111 inhibited HGF-dependent colony formation by 78% (Fig. 4E). Finally, in a HGF-induced branching morphogenesis assay using SV40 T-antigen-transformed LOC

human kidney epithelial cell spheroids (23) and increasing antibody concentrations, ARGX-111 significantly inhibited HGF-induced branched tubule formation already at a 1:1 molar ratio with recombinant HGF (Fig. 4F).

ARGX-111 inhibits HGF-independent MET activity by promoting kinase-independent receptor down-regulation

We next determined whether ARGX-111 could affect HGF-independent MET activity in tumor cells displaying constitutive MET activation. In phospho-MET ELISA assays, ARGX-111 showed dose-dependent inhibition of MET auto-phosphorylation in both MKN-45 cells (IC_{50} = 0.2 nM, I_{MAX} = 63%; Fig. 5A) and EBC-1 human lung carcinoma cells (IC_{50} = 12.7 nM, I_{MAX} = 69%; Fig. 5B). Flow cytometry analysis of MET expression revealed that ARGX-111 promoted a rapid decrease of MET expression levels in both MKN-45 cells (Fig. 5C) and EBC-1 cells (Fig. 5D). Interestingly, this effect was also observed in MDA-MB-231 human mammary carcinoma cells (Fig. 3E), which express normal MET levels and retain ligand sensitivity. ARGX-111-mediated MET down-regulation was dose-dependent, reaching its maximal effect already at 10 nM (Fig. 5F). Western blot analysis of conditioned medium (Suppl. Fig. S6A) and of cell lysates (Suppl. Fig. S6B) demonstrated that ARGX-111 does not promote receptor shedding but reduces total MET protein levels, suggesting that antibody binding to MET results in receptor internalization followed by protein degradation. ARGX-111-induced MET-down-regulation also occurred in the presence of a highly specific MET tyrosine kinase inhibitor (JNJ-38877605; ref. 32) in MKN-45 (Fig. 5G), EBC-1 (Fig. 5H) and MDA-MB-231 cells (Fig. 5I), suggesting that this process does not require MET kinase activity. In contrast, MET kinase inhibition did block HGF-induced MET internalization in MDA-MB-231 cells (Fig. 5I). Western blot analysis confirmed that the concentration of JNJ-38877605 used in these experiments achieved complete MET kinase blockade in all cells (Suppl. Fig 6C).

ARGX-111 kills MET-expressing cancer cells in the presence of NK cells

We investigated whether ARGX-111 could kill cancer cells by ADCC using a representative panel of human tumor cell lines expressing different MET levels. Cells were incubated with increasing concentrations of ARGX-111 (0-1,000 nM) in the presence of NK cells, and tumor cell lysis was determined by a standard ^{51}Cr-release assay. An irrelevant IgG1 and the fucosylated G52 antibody were used as controls. Each assay was repeated using effector cells derived from 3 different healthy donors (Suppl. Tab. S6). This analysis revealed that ARGX-111 induces dose-dependent lysis of all tumor cell lines tested with an efficacy directly proportional to MET protein expression levels. The fucosylated G52 antibody displayed only a modest ADCC activity on MKN-45 cells, which express very high MET levels, but did not have any effect on the other cell lines tested (Suppl. Fig. S7A). We also analyzed ARGX-111-induced antibody-dependent cellular phagocytosis (ADCP) using MKN-45 cells or 786-O human renal cell carcinoma cells and human monocyte-derived macrophages. Consistent with our finding that afucosylation does not significantly change antibody affinity for FcγRI (Suppl. Tab. S4), ARGX-111 did not display increased ADCP compared to G52 in any condition tested (Suppl. Fig. S7B).

MET-targeted ADCC kills mammary carcinoma stem cells

The results obtained in the orthotopic mammary carcinoma models indicate that MET-targeted ADCC impairs the ability of CTCs to colonize distant organs and to give rise to metastases. Since only tumor cells with stem-like characteristics are competent to originate secondary colonies, we hypothesized that the mammary carcinoma stem cell population may express MET. To test this hypothesis, we analyzed co-expression of MET with established breast cancer stem cell markers (33) in MDA-MB-231 tumors as well as in a vital library of patient-derived breast xenografts (CRCM tumors; 25) generated by implantation of primary mammary carcinomas into immunodeficient mice (Fig. 6A). Interestingly, all triple negative tumors from this library expressed MET (Fig. 6B). Flow cytometry

analysis of CD24, CD44 and MET unveiled that the majority of cells in the $CD44^{+}/CD24^{lo}$ population express MET in both the MDA-MB-231 cell line (99%) and the primary breast carcinoma samples (78-98%; Suppl. Tab. S7). Similarly, dual staining with AldeFluor™ reaction and anti-MET antibodies revealed that ALDH-1-positive tumor cells express MET in all samples analyzed (Fig. 7A). Prompted by these data, we determined whether MET-targeted ADCC could kill mammary carcinoma stem cells in vitro. To this end, cells derived from MDA-MB-231, CRCM168, CRCM174 and CRCM389 tumors were stained with AldeFluor™ and then sorted by FACS. Sorted cells were incubated with increasing ARGX-111 concentrations (0-667 nM) in the presence of bioluminescent ADCC reporter cells (34), and ADCC was determined by analyzing luciferase activity. Remarkably, ARGX-111 promoted dose-dependent ADCC of all stem cell populations analyzed (Fig. 7B). We conclude that MET-targeted ADCC may be an effective method to eliminate breast cancer stem cells.

DISCUSSION

HGF and its receptor MET have been attracting increasing interest in the last two decades as appealing targets for cancer therapy. This interest has led to the development of numerous targeted drugs, some of which have reached the clinic. The initial enthusiasm has been partially mitigated, however, by the realization that anti-HGF/MET drugs display cytostatic rather than cytotoxic activity in most systems, including cell-based assays, mouse models of cancer and oncological patients. In this study we report the engineering of an antagonistic anti-MET antibody that, in addition to inhibiting HGF/MET signaling, kills MET-expressing tumor cells by enhanced ADCC. The data presented here suggest that depleting MET-positive cancer cells is therapeutically more effective than simply inhibiting HGF/MET signaling.

These results must be interpreted at the light of the role played by MET in cancer biology. It has been shown that tumors take advantage of HGF/MET signaling in 2 different situations, determined by the number of c-*MET* gene copies contained in their genome (22). Tumors bearing normal c-*MET* gene copy number exploit paracrine HGF stimulation to proliferate in adverse environmental conditions and to invade adjacent tissues, but do not strictly depend on HGF/MET signaling for their own survival. In this setting, inhibition of HGF/MET signaling attenuates proliferation and invasion, but does not eliminate MET-expressing cancer cells per se. On the other hand, tumors displaying high grade focal c-*MET* amplification totally rely on constitutive HGF-independent MET signaling, resulting from MET protein overexpression, to sustain their proliferation and EMT phenotype (35, 36). In these tumors, MET inhibition leads to G1 arrest and to transient reversion of EMT; however, both proliferation and EMT can be resumed upon removal of MET blockade (20). Therefore, whether we are hindering HGF-mediated oncogenic 'expedience' in tumors bearing normal c-*MET* gene copy number or MET-dependent

oncogenic 'addiction' in c-*MET*-amplified lesions, we are temporarily preventing tumor cells to carry out their malignant program, but we are not eradicating them.

This notion acquires high therapeutic relevance in light of the emerging evidence that MET is expressed and functionally required in the stem cell compartment of several tumor types, including head and neck carcinoma (37), colorectal carcinoma (38), prostate cancer (39), breast cancer (40), and glioblastoma multiforme (41). In analogy with normal tissue stem cells, cancer stem cells represent a multi-potent tumor cell sub-population that possesses the ability to replicate indefinitely and to give rise to secondary tumor colonies with the full differentiation spectrum of the primary lesion. Circulating cancer cells with stem-like characteristics are the only cell type that can give rise to metastases and are often drug-resistant (42). Following therapy interruption, residual cancer stem cells that survived treatment may resume their proliferative cycle, reconquer space in the host organism, and give rise to malignant lesions, resulting in new metastases or tumor recurrence (43). From a therapeutic viewpoint, killing rather than simply inhibiting the proliferation of cancer stem cells may be associated with a greater patient benefit.

The possibility to intercept MET-positive CTCs with stem-like properties generates a new paradigm for the treatment of MET-positive tumors. So far, MET-targeted therapy has been envisioned either for causing the regression of established HGF/MET-dependent lesions or for overcoming HGF/MET-driven resistance to a second anticancer drug (44). The data presented here suggest that these strategies may not exploit the full therapeutic potential of an ADCC-enhanced anti-MET antibody, and point at the neo-adjuvant and adjuvant settings as valid alternative approaches. Indeed, CTCs are ultimately responsible for tumor recurrence or metastasis onset following surgery, independently of how well the original lesion has responded to a previous therapy. Based on the results obtained in our neo-adjuvant and adjuvant orthotopic breast cancer models, it would be reasonable to expect that eradication of CTCs by MET-targeted ADCC is associated with prolonged disease-free survival. Importantly, this opportunity is

unique to an ADCC-enhanced anti-MET antibody. In fact, inhibition of HGF/MET signaling using a conventional HGF/MET-targeted drug, whether an antibody or a small molecule, would probably be able to prevent the escape of cancer cells from a primary lesion, but would have no effect on the survival of metastasis-initiating cells once they are in circulation, especially if these cells have become resistant to anoikis during their journey from the home epithelium to the breakout vessel.

Although MET plays its most relevant physiological role during embryo development and remains mostly silent during the adult stage, it is widely expressed in epithelial and endothelial tissues of virtually all organs. This broad expression pattern could raise the concern that MET-targeted ADCC may cause damage to normal tissues, resulting in systemic toxicity. However, toxicological studies conducted in cynomolgus monkeys (*Macaca fascicularis*) indicate that this is not the case. In fact, while ARGX-111 does not cross-react with mouse MET, it binds with high affinity to simian MET and to simian FcγRIIIa (Suppl. Tab. S4). In a large study involving 40 adult animals, the no-observed adverse event level (NOAEL) of ARGX-111 corresponded to a dose of 30 mg/kg administered weekly (data on file). These results suggest that MET-targeted ADCC may be well tolerated by normal tissues expressing MET and may therefore not interfere with housekeeping physiological functions at doses that are active against MET-dependent tumors. More definitive data on ARGX-111 safety will emerge from the phase I study that has started in January 2014 (NCT02055066).

ACKNOWLEDGEMENTS

We thank Brigitte Bonnin and John Wijdenes for the ADCP and ADCC assays, Sylvie Richelme for HGF-dependent assays, Sjudry-llona Osepa for llama-human chimera construction and U-protein Express for production and purification of antibodies.

REFERENCES

1. Trusolino L, Bertotti A, Comoglio PM. MET signalling: principles and functions in development, organ regeneration and cancer. *Nat Rev Mol Cell Biol.* 2010; 11:834-848.

2. Nakamura T, Mizuno S. The discovery of hepatocyte growth factor (HGF) and its significance for cell biology, life sciences and clinical medicine. *Proc Jpn Acad Ser B Phys Biol Sci.* 2010; 86:588-610.

3. Birchmeier C, Birchmeier W, Gherardi E, Vande Woude GF. Met, metastasis, motility and more. *Nat Rev Mol Cell Biol.* 2003; 4:915-925.

4. Comoglio PM, Trusolino L. Invasive growth: from development to metastasis. *J Clin Invest.* 2002; 109:857-862.

5. Nakamura T, Mizuno S. The discovery of hepatocyte growth factor (HGF) and its significance for cell biology, life sciences and clinical medicine. *Proc Jpn Acad Ser B Phys Biol Sci.* 2010; 86:588-610.

6. Trusolino L, Comoglio PM. Scatter-factor and semaphorin receptors: cell signalling for invasive growth. *Nat Rev Cancer* 2002; 2:289-300.

7. To CT, Tsao MS. The roles of hepatocyte growth factor/scatter factor and met receptor in human cancers. *Oncol Rep.* 1998; 5:1013-1024.

8. You WK, McDonald DM. The hepatocyte growth factor/c-Met signaling pathway as a therapeutic target to inhibit angiogenesis. *BMB Rep.* 2008; 41:833-839.

9. Gherardi E, Birchmeier W, Birchmeier C, Vande Woude G. Targeting MET in cancer: rationale and progress. *Nat Rev Cancer* 2012; 12:89-103.

10. Cappuzzo F, Marchetti A, Skokan M, Rossi E, Gajapathy S, Felicioni L, Del Grammastro M, Sciarrotta MG, Buttitta F, Incarbone M, Toschi L, Finocchiaro G, Destro A, Terracciano L, Roncalli M, Alloisio M, Santoro A, Varella-Garcia M. Increased MET gene copy number negatively affects survival of surgically resected non-small-cell lung cancer patients. *J Clin Oncol.* 2009; 27:1667-1674.

11. De Oliveira AT, Matos D, Logullo AF, DA Silva SR, Neto RA, Filho AL, Saad SS. MET Is highly expressed in advanced stages of colorectal cancer and indicates worse prognosis and mortality. *Anticancer Res.* 2009; 29:4807-4811.

12. Zagouri F, Bago-Horvath Z, Rössler F, Brandstetter A, Bartsch R, Papadimitriou CA, Dimitrakakis C, Tsigginou A, Papaspyrou I, Giannos A, Dimopoulos MA, Filipits M. High MET expression is an adverse prognostic factor in patients with triple-negative breast cancer. *Br J Cancer* 2013; 108:1100-1105.

13. Tuynman JB, Lagarde SM, Ten Kate FJ, Richel DJ, van Lanschot JJ. Met expression is an independent prognostic risk factor in patients with oesophageal adenocarcinoma. *Br J Cancer* 2008; 98:1102-1108.

14. Graziano F, Galluccio N, Lorenzini P, Ruzzo A, Canestrari E, D'Emidio S, Catalano V, Sisti V, Ligorio C, Andreoni F, Rulli E, Di Oto E, Fiorentini G, Zingaretti C, De Nictolis M, Cappuzzo F, Magnani M. Genetic activation of the MET pathway and prognosis of patients with high-risk, radically resected gastric cancer. *J Clin Oncol.* 2011; 29:4789-4795.

15. Rocci A, Gambella M, Aschero S, Baldi I, Trusolino L, Cavallo F, Gay F, Larocca A, Magarotto V, Omedè P, Isaia G, Bertotti A, Liberati AM, Catalano L, De Rosa L, Musto P, Vallone R, Falcone A, Drandi D, Ladetto M, Comoglio PM, Boccadoro M, Palumbo A. MET dysregulation is a hallmark of aggressive disease in multiple myeloma patients. *Br J Haematol.* 2014; 164:841-850.

16. Olmez OF, Cubukcu E, Evrensel T, Kurt M, Avci N, Tolunay S, Bekar A, Deligonul A, Hartavi M, Alkis N, Manavoglu O. The immunohistochemical expression of c-Met is an independent predictor of survival in patients with glioblastoma multiforme. Clin Transl Oncol. 2014; 16:173-177.

17. Underiner TL, Herbertz T, Miknyoczki SJ. Discovery of small molecule c-Met inhibitors: Evolution and profiles of clinical candidates. *Anticancer Agents Med Chem.* 2010; 10:7-27.

18. Cecchi F, Rabe DC, Bottaro DP. Targeting the HGF/Met signaling pathway in cancer therapy. *Expert Opin Ther Targets* 2012; 16:553-572.

19. Smyth EC, Sclafani F, Cunningham D. Emerging molecular targets in oncology: clinical potential of MET/hepatocyte growth-factor inhibitors. Onco Targets Ther. 2014; 7:1001-1014.

20. Bertotti A, Burbridge MF, Gastaldi S, Galimi F, Torti D, Medico E, Giordano S, Corso S, Rolland-Valognes G, Lockhart BP, Hickman JA, Comoglio PM, Trusolino L. Only a subset of Met-activated pathways are required to sustain oncogene addiction. *Sci Signal.* 2009; 2:ra80.

21. Lai AZ, Cory S, Zhao H, Gigoux M, Monast A, Guiot MC, Huang S, Tofigh A, Thompson C, Naujokas M, Marcus VA, Bertos N, Sehat B, Perera RM, Bell ES, Page BD, Gunning PT, Ferri LE, Hallett M, Park M. Dynamic reprogramming of signaling upon met inhibition reveals a mechanism of drug resistance in gastric cancer. *Sci Signal.* 2014; 7:ra38.

22. Comoglio PM, Giordano S, Trusolino L. Drug development of MET inhibitors: targeting oncogene addiction and expedience. *Nat Rev Drug Discov.* 2008; 7:504-516.

23. Michieli P, Cavassa S, Basilico C, De Luca A, Mazzone M, Asti C, Chiusaroli R, Guglielmi M, Bossù P, Colotta F, Caselli G, Comoglio PM. An HGF-MSP chimera disassociates the trophic properties of scatter factors from their pro-invasive activity. *Nat Biotechnol.* 2002; 20:488-495.

24. Basilico C, Hultberg A, Blanchetot C, de Jonge N, Festjens E, Hanssens V, Osepa SI, De Boeck G, Mira A, Cazzanti M, Morello V, Dreier T, Saunders M, de Haard H, Michieli P. Four individually druggable MET hotspots mediate HGF-driven tumor progression. *J Clin Invest.* 2014; 124:3172-3186.

25. Charafe-Jauffret E, Ginestier C, Bertucci F, Cabaud O, Wicinski J, Finetti P, Josselin E, Adelaide J, Nguyen TT, Monville F, Jacquemier J, Thomassin-Piana J, Pinna G, Jalaguier A, Lambaudie E, Houvenaeghel G, Xerri L, Harel-Bellan A, Chaffanet M, Viens P, Birnbaum D. ALDH1-positive cancer stem cells predict engraftment of primary breast tumors and are governed by a common stem cell program. *Cancer Res.* 2013; 73:7290-7300.

26. Armour KL, Clark MR, Hadley AG, Williamson LM. Recombinant human IgG molecules lacking Fcgamma receptor I binding and monocyte triggering activities. *Eur J Immunol.* 1999; 29:2613-2624.

27. Lazar GA, Dang W, Karki S, Vafa O, Peng JS, Hyun L, Chan C, Chung HS, Eivazi A, Yoder SC, Vielmetter J, Carmichael DF, Hayes RJ, Dahiyat BI. Engineered antibody Fc variants with enhanced effector function. *Proc Natl Acad Sci USA* 2006; 103:4005-4010.

28. Martens T, Schmidt NO, Eckerich C, Fillbrandt R, Merchant M, Schwall R, Westphal M, Lamszus K. A novel one-

armed anti-c-Met antibody inhibits glioblastoma growth in vivo. *Clin Cancer Res.* 2006; 12:6144-6152.

29. Pennacchietti S, Cazzanti M, Bertotti A, Rideout WM 3rd, Han M, Gyuris J, Perera T, Comoglio PM, Trusolino L, Michieli P. Microenvironment-derived HGF overcomes genetically determined sensitivity to anti-MET drugs. Cancer Res. 2014; 74:6598-6609.

30. Vaccaro C, Bawdon R, Wanjie S, Ober RJ, Ward ES. Divergent activities of an engineered antibody in murine and human systems have implications for therapeutic antibodies. *Proc Natl Acad Sci USA* 2006; 103:18709-18714.

31. Masuda K, Kubota T, Kaneko E, Iida S, Wakitani M, Kobayashi-Natsume Y, Kubota A, Shitara K, Nakamura K. Enhanced binding affinity for FcgammaRIII of fucose-negative antibody is sufficient to induce maximal antibody-dependent cellular cytotoxicity. *Mol Immunol.* 2007; 44:3122-3131.

32. Basilico C, Pennacchietti S, Vigna E, Chiriaco C, Arena S, Bardelli A, Valdembri D, Serini G, Michieli P. Tivantinib (ARQ197) displays cytotoxic activity that is independent of its ability to bind MET. *Clin Cancer Res.* 2013; 19:2381-2392.

33. Iqbal J, Chong PY, Tan PH. Breast cancer stem cells: an update. *J Clin Pathol.* 2013; 66:485-490.

34. Parekh BS, Berger E, Sibley S, Cahya S, Xiao L, LaCerte MA, Vaillancourt P, Wooden S, Gately D. Development and validation of an antibody-dependent cell-mediated cytotoxicity-reporter gene assay. *MAbs* 2012; 4:310-318.

35. Smolen GA, Sordella R, Muir B, Mohapatra G, Barmettler A, Archibald H, Kim WJ, Okimoto RA, Bell DW, Sgroi DC, Christensen JG, Settleman J, Haber DA. Amplification of MET may identify a subset of cancers with extreme sensitivity to the selective tyrosine kinase inhibitor PHA-665752. *Proc Natl Acad Sci USA* 2006; 103:2316-2321.

36. McDermott U, Sharma SV, Dowell L, Greninger P, Montagut C, Lamb J, Archibald H, Raudales R, Tam A, Lee D, Rothenberg SM, Supko JG, Sordella R, Ulkus LE, Iafrate AJ, Maheswaran S, Njauw CN, Tsao H, Drew L, Hanke JH, Ma XJ, Erlander MG, Gray NS, Haber DA, Settleman J. Identification of genotype-correlated sensitivity to selective kinase inhibitors by using high-throughput tumor cell line profiling. *Proc Natl Acad Sci USA* 2007;

104:19936-19941.

37. Lim YC, Kang HJ, Moon JH. C-Met pathway promotes self-renewal and tumorigenecity of head and neck squamous cell carcinoma stem-like cell. *Oral Oncol.* 2014; 50:633-639.

38. Luraghi P, Reato G, Cipriano E, Sassi F, Orzan F, Bigatto V, De Bacco F, Menietti E, Han M, Rideout WM 3rd, Perera T, Bertotti A, Trusolino L, Comoglio PM, Boccaccio C. MET signaling in colon cancer stem-like cells blunts the therapeutic response to EGFR inhibitors. *Cancer Res.* 2014; 74:1857-1869.

39. Nishida S, Hirohashi Y, Torigoe T, Inoue R, Kitamura H, Tanaka T, Takahashi A, Asanuma H, Masumori N, Tsukamoto T, Sato N. Prostate cancer stem-like cells/cancer-initiating cells have an autocrine system of hepatocyte growth factor. *Cancer Sci.* 2013; 104:431-436.

40. Baccelli I, Schneeweiss A, Riethdorf S, Stenzinger A, Schillert A, Vogel V, Klein C, Saini M, Bäuerle T, Wallwiener M, Holland-Letz T, Höfner T, Sprick M, Scharpff M, Marmé F, Sinn HP, Pantel K, Weichert W, Trumpp A. Identification of a population of blood circulating tumor cells from breast cancer patients that initiates metastasis in a xenograft assay. *Nat Biotechnol.* 2013; 31:539-544..

41. De Bacco F, Casanova E, Medico E, Pellegatta S, Orzan F, Albano R, Luraghi P, Reato G, D'Ambrosio A, Porrati P, Patanè M, Maderna E, Pollo B, Comoglio PM, Finocchiaro G, Boccaccio C. The MET oncogene is a functional marker of a glioblastoma stem cell subtype. *Cancer Res.* 2012; 72:4537-4550.

42. Meacham CE, Morrison SJ. Tumour heterogeneity and cancer cell plasticity. *Nature* 2013; 501:328-337.

43. Holohan C, Van Schaeybroeck S, Longley DB, Johnston PG. Cancer drug resistance: an evolving paradigm. *Nat Rev Cancer* 2013; 13:714-726.

44. Parikh RA, Wang P, Beumer JH, Chu E, Appleman LJ. The potential roles of hepatocyte growth factor (HGF)-MET pathway inhibitors in cancer treatment. *OncoTargets Ther.* 2014; 7:969-983.

FIGURE LEGENDS

Figure 1. ADCC enhancement results in improved anti-tumor activity in both HGF-dependent and -independent xenograft models. (A) Mice bearing U87-MG tumors were and randomly assigned to 3 treatment arms (irrelevant IgG1, WT52-E, WT52-D; 5 mg/kg), and tumor volume was monitored over time. Statistical significance was calculated by a Student's T-test. (B) Weight analysis of the tumors explanted at the end of the experiment described in A. (C) Mice bearing MKN-45 tumors were randomly assigned to 3 treatment arms as above (IgG1, WT52-E, WT52-D; 1 mg/kg), and tumor volume was monitored over time. (D) Mice bearing MKN-45 tumors were injected with a single bolus (5 mg/kg) of WT52-E or irrelevant IgG1, and tumors were analyzed by immunohistochemistry 24 hours later using anti-phospho-MET or anti-total MET antibodies. Magnification: 100X.

Figure 2. MET-targeted ADCC inhibits tumor growth and metastasis in a neo-adjuvant orthotopic mammary carcinoma model. (A) Schematic protocol representation. CTCs, circulating tumor cells. (B) Analysis of tumor volume over time. Statistical significance was calculated by a Student's T-test. (C) Pulmonary metastases as assessed by lung bioluminescence (BL). (D) Bone metastases as assessed by femur bioluminescence. (E) CTCs over time as assessed by blood luciferase activity. (F) At autopsy, CTC number correlated directly with the extent of metastatic dissemination and inversely with anti-MET treatment.

Figure 3. Adjuvant MET-targeted ADCC suppresses metastasis by eliminating circulating tumor cells. (A) Schematic protocol representation. CTCs, circulating tumor cells. (B) Analysis of CTC number over time. Statistical significance was calculated by a Student's T-test. (C) CTC number at autopsy. (D) Whole

body bioluminescence (BL) at autopsy. (E) Lung bioluminescence at autopsy. (F) Femur bioluminescence at autopsy.

Figure 4. ARGX-111 inhibits HGF-dependent MET activity by competing with HGF for binding to MET. (A) The ability of ARGX-111 or an irrelevant IgG1 to compete with HGF for binding to MET was determined by ELISA. Data are expressed as % HGF binding in the absence of antibody. (B) The ability of ARGX-111 to inhibit HGF-induced MET auto-phosphorylation was determined using A549 cells. Data are expressed as % phospho-MET levels relative to cells stimulated with HGF alone. (C) Same as in B but using NCI-H1437 cells. (D) Boyden chamber migration assay using A549 cells. Data are expressed as % migrating cells relative to total cell number. Statistical significance was calculated by a Student's T-test. (E) Anchorage-independent assay using NCI-H1437 cells. Colony number is expressed as % colonies relative to cells stimulated with HGF alone. (F) LOC cell spheroids were seeded in collagen and then stimulated with a fixed dose of recombinant HGF in the presence of increasing concentrations of ARGX-111. Branching morphogenesis was assessed by microscopy. Magnification: 100X.

Figure 5. ARGX-111 inhibits HGF-independent MET activity by promoting receptor down-regulation. (A) The ability of ARGX-111 to inhibit HGF-independent MET auto-phosphorylation was determined using MKN-45 cells. Data are expressed as % phospho-MET levels compared to untreated (UT) cells. (B) Same as in A but using EBC-1 cells. (C) Flow cytometry analysis of ARGX-111-mediated MET down-regulation in MKN-45 cells. Data are expressed as % MET levels compared to untreated cells. (D) Same as in C but using EBC-1 cells. (E) Same as in C but using MDA-MB-231 cells. (F) Dose-response analysis of ARGX-111-mediated MET down-regulation in MKN-45 cells. (G-I) Flow cytometry analysis of ARGX-111- or HGF-mediated MET down-regulation in the presence or absence of JNJ-38877605, a highly selective MET tyrosine kinase inhibitor. Statistical significance was calculated by a Student's T-test.

Figure 6. MET expression in patient-derived primary breast cancer xenografts. (A) Tumor cell suspensions obtained by enzymatic digestion of patient-derived mammary carcinoma samples are injected orthotopically into the mammary fat pad of a NOG mouse that has been previously humanized using human mammary fibroblasts (hMFS). Once engrafted, tumors are propagated from mouse to mouse using the same technique. (B) MET expression analysis of cells derived from the vital xenograft library described in A. TNBC, triple-negative breast cancer.

Figure 7. MET-targeted ADCC kills mammary carcinoma stem cells. (A) Flow cytometry analysis of MET expression in ALDH-1^+ mammary carcinoma cells. (B) ADCC assay using ALDH-1-sorted cells derived from enzymatic digestion of the tumors described in A. ADCC was determined using bioluminescent ADCC reporter cells. LUC, luciferase; AU, arbitrary units.

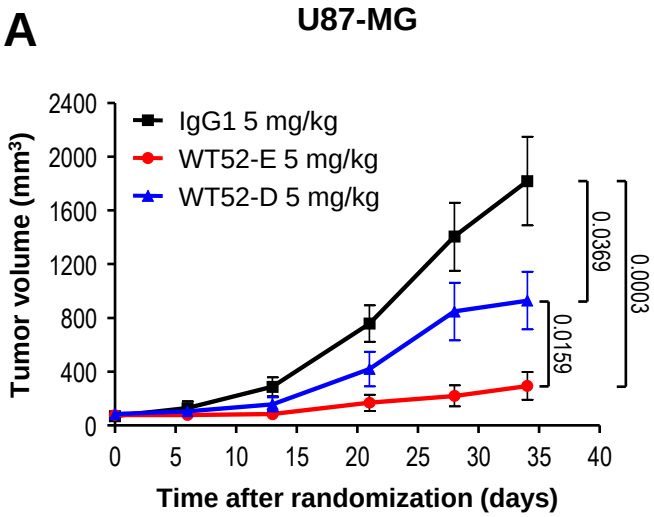
A
U87-MG
IgG1 5 mg/kg
WT52-E 5 mg/kg
WT52-D 5 mg/kg
Tumor volume (mm³)
Time after randomization (days)
0.0369
0.0003
0.0159

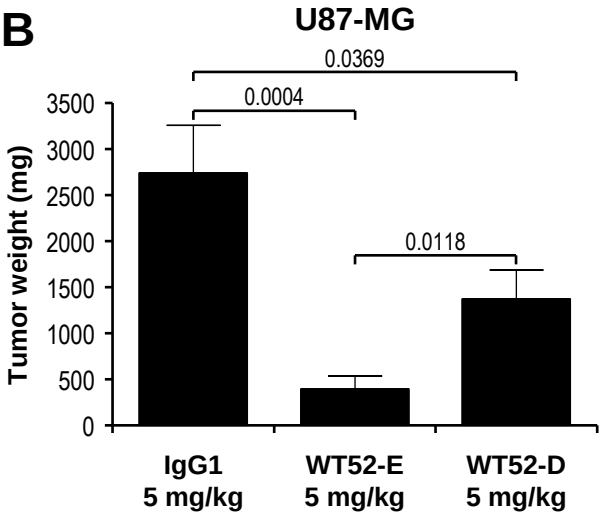
B
U87-MG
Tumor weight (mg)
0.0369
0.0004
0.0118
IgG1 5 mg/kg
WT52-E 5 mg/kg
WT52-D 5 mg/kg

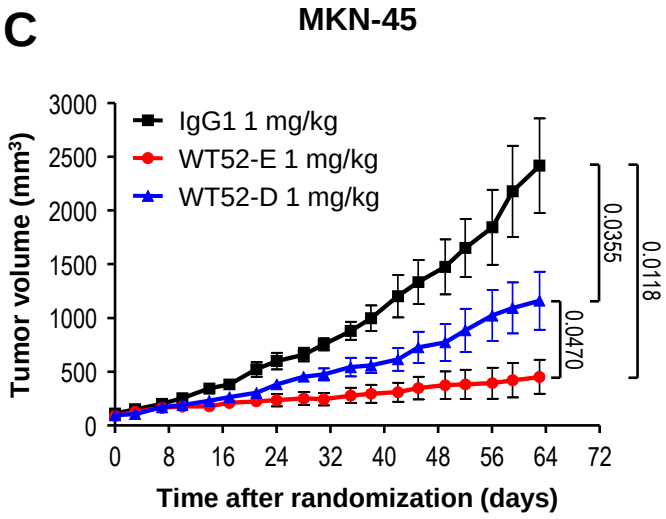
C
MKN-45
IgG1 1 mg/kg
WT52-E 1 mg/kg
WT52-D 1 mg/kg
Tumor volume (mm³)
Time after randomization (days)
0.0355
0.0118
0.0470

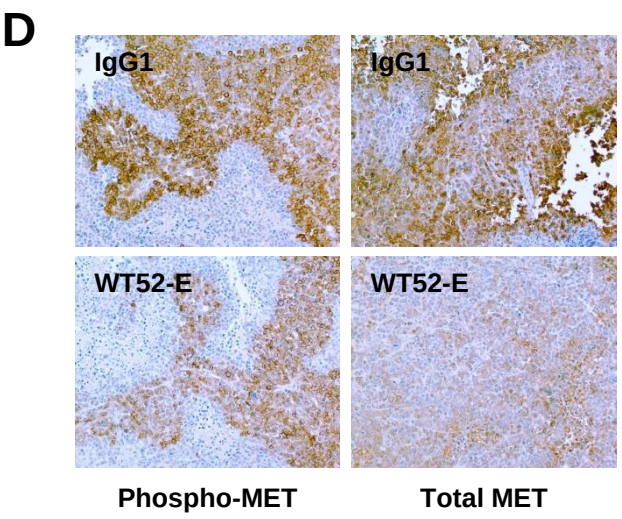
D
IgG1
IgG1
WT52-E
WT52-E
Phospho-MET
Total MET

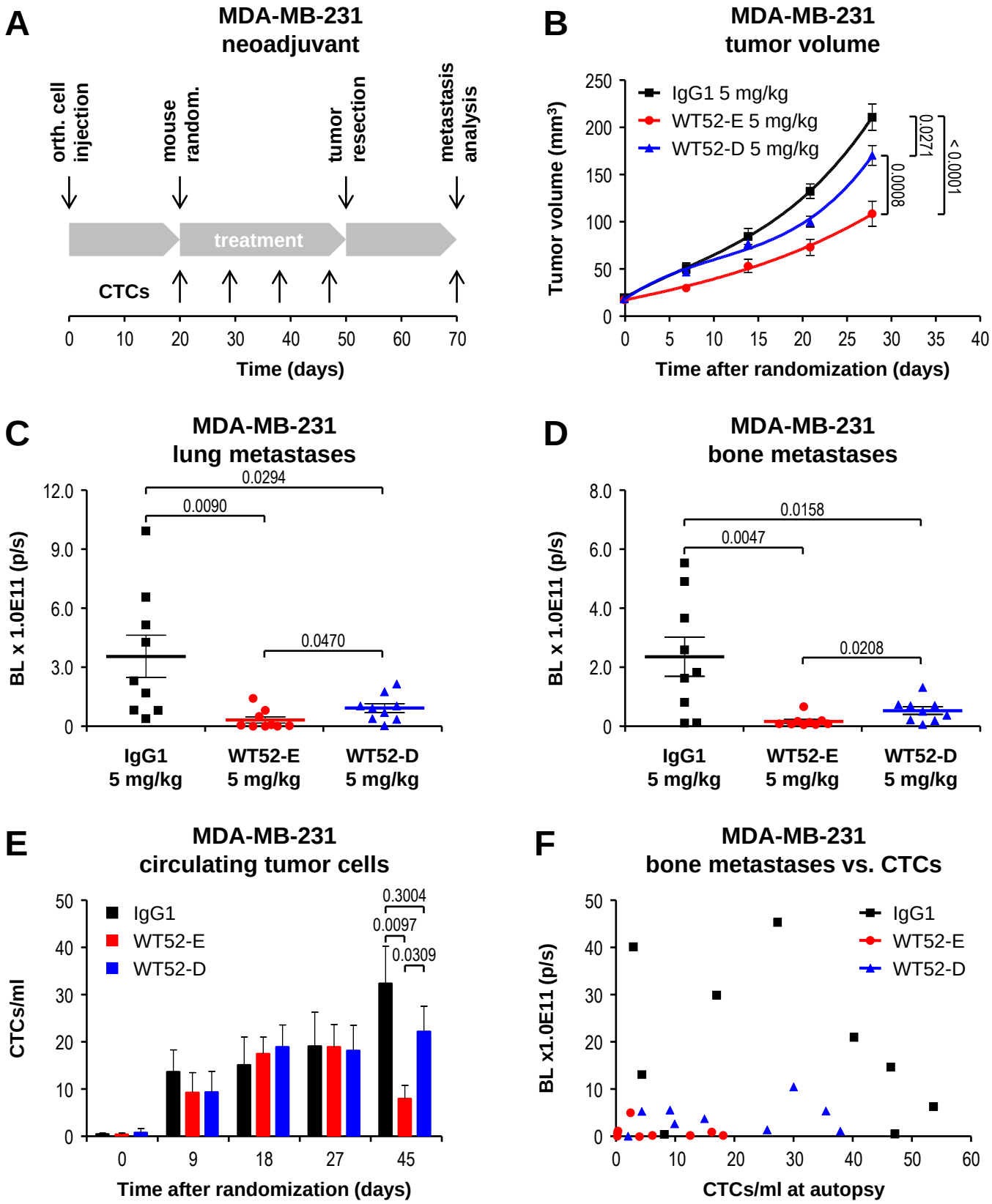
A
MDA-MB-231
neoadjuvant
orth. cell injection
mouse random.
tumor resection
metastasis analysis
treatment
CTCs
0 10 20 30 40 50 60 70
Time (days)
B
MDA-MB-231
tumor volume
IgG1 5 mg/kg
WT52-E 5 mg/kg
WT52-D 5 mg/kg
Tumor volume (mm³)
0 50 100 150 200 250
0 5 10 15 20 25 30 35 40
Time after randomization (days)
0.0271
0.0008
< 0.0001
C
MDA-MB-231
lung metastases
BL x 1.0E11 (p/s)
0 3.0 6.0 9.0 12.0
0.0294
0.0090
0.0470
IgG1 5 mg/kg
WT52-E 5 mg/kg
WT52-D 5 mg/kg
D
MDA-MB-231
bone metastases
BL x 1.0E11 (p/s)
0 2.0 4.0 6.0 8.0
0.0158
0.0047
0.0208
IgG1 5 mg/kg
WT52-E 5 mg/kg
WT52-D 5 mg/kg
E
MDA-MB-231
circulating tumor cells
IgG1
WT52-E
WT52-D
CTCs/ml
0 10 20 30 40 50
0.3004
0.0097
0.0309
0 9 18 27 45
Time after randomization (days)
F
MDA-MB-231
bone metastases vs. CTCs
IgG1
WT52-E
WT52-D
BL x1.0E11 (p/s)
0 10 20 30 40 50
0 10 20 30 40 50 60
CTCs/ml at autopsy

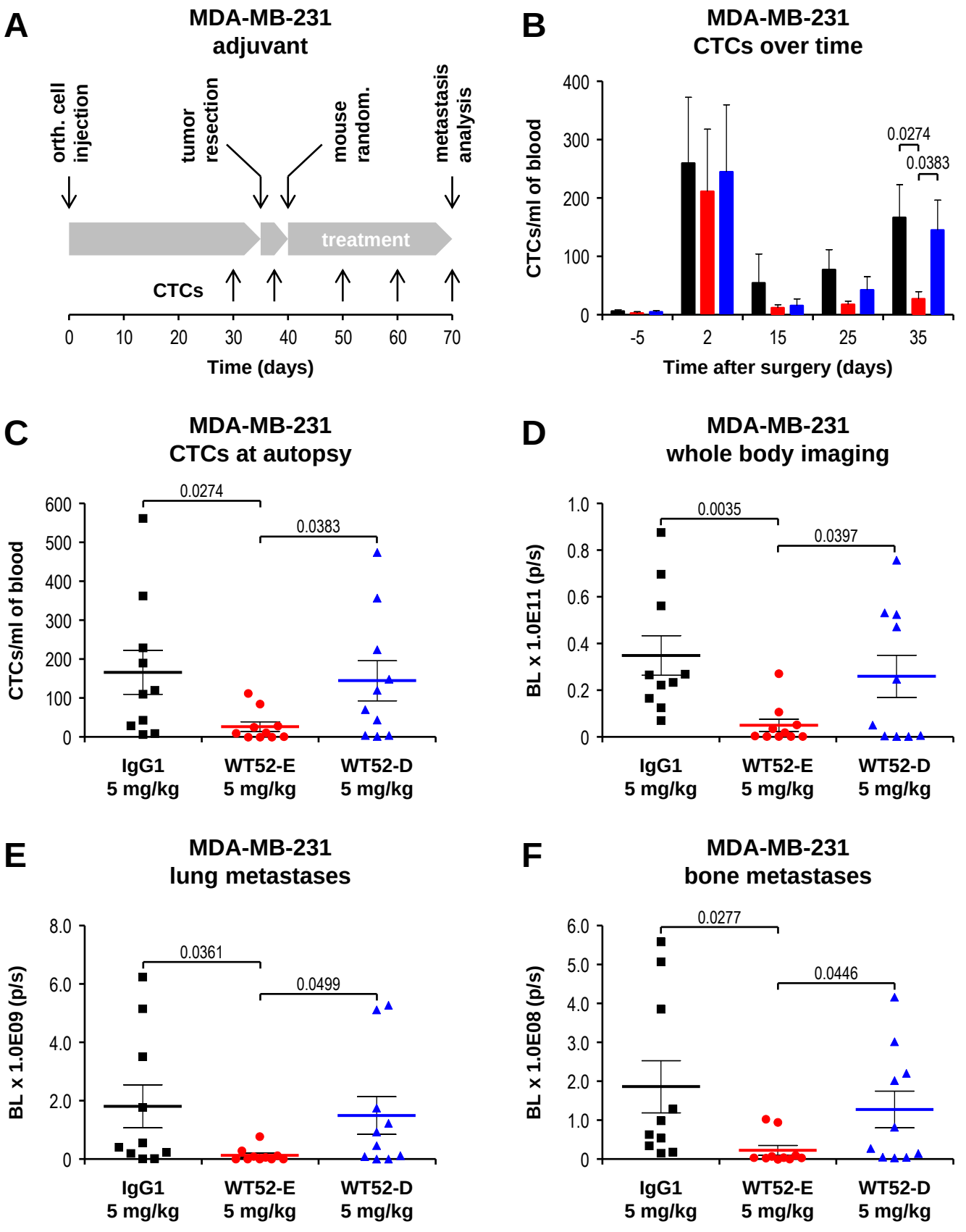
A
MDA-MB-231
adjuvant
orth. cell injection
tumor resection
mouse random.
metastasis analysis
treatment
CTCs
0
10
20
30
40
50
60
70
Time (days)
B
MDA-MB-231
CTCs over time
CTCs/ml of blood
400
300
200
100
0
0.0274
0.0383
-5
2
15
25
35
Time after surgery (days)
C
MDA-MB-231
CTCs at autopsy
CTCs/ml of blood
600
500
400
300
200
100
0
0.0274
0.0383
IgG1 5 mg/kg
WT52-E 5 mg/kg
WT52-D 5 mg/kg
D
MDA-MB-231
whole body imaging
BL x 1.0E11 (p/s)
1.0
0.8
0.6
0.4
0.2
0
0.0035
0.0397
IgG1 5 mg/kg
WT52-E 5 mg/kg
WT52-D 5 mg/kg
E
MDA-MB-231
lung metastases
BL x 1.0E09 (p/s)
8.0
6.0
4.0
2.0
0
0.0361
0.0499
IgG1 5 mg/kg
WT52-E 5 mg/kg
WT52-D 5 mg/kg
F
MDA-MB-231
bone metastases
BL x 1.0E08 (p/s)
6.0
5.0
4.0
3.0
2.0
1.0
0
0.0277
0.0446
IgG1 5 mg/kg
WT52-E 5 mg/kg
WT52-D 5 mg/kg

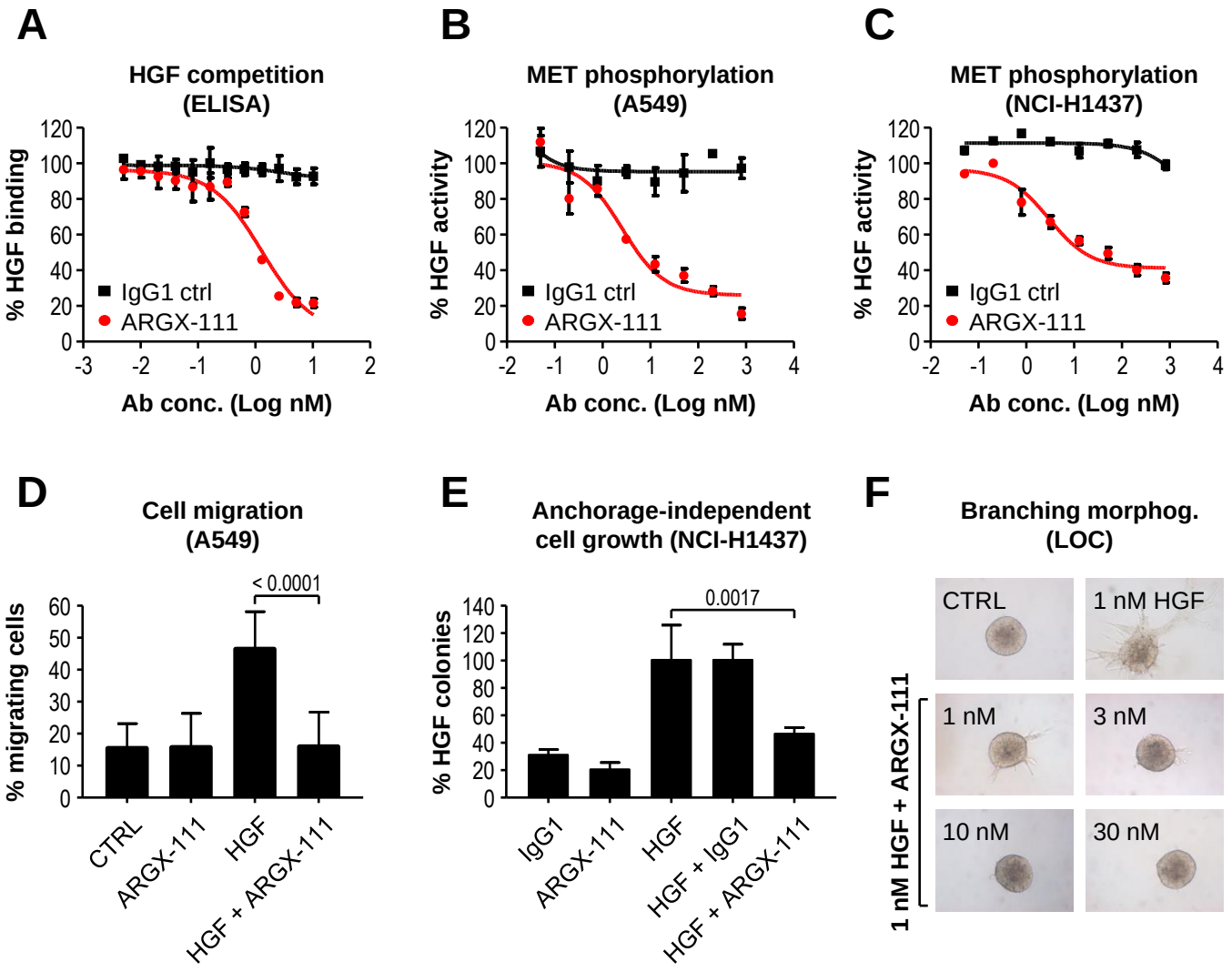
A
HGF competition (ELISA)
% HGF binding
IgG1 ctrl
ARGX-111
Ab conc. (Log nM)
B
MET phosphorylation (A549)
% HGF activity
IgG1 ctrl
ARGX-111
Ab conc. (Log nM)
C
MET phosphorylation (NCI-H1437)
% HGF activity
IgG1 ctrl
ARGX-111
Ab conc. (Log nM)
D
Cell migration (A549)
% migrating cells
< 0.0001
CTRL
ARGX-111
HGF
HGF + ARGX-111
E
Anchorage-independent cell growth (NCI-H1437)
% HGF colonies
0.0017
IgG1
ARGX-111
HGF
HGF + IgG1
HGF + ARGX-111
F
Branching morphog. (LOC)
CTRL
1 nM HGF
1 nM
3 nM
10 nM
30 nM
1 nM HGF + ARGX-111

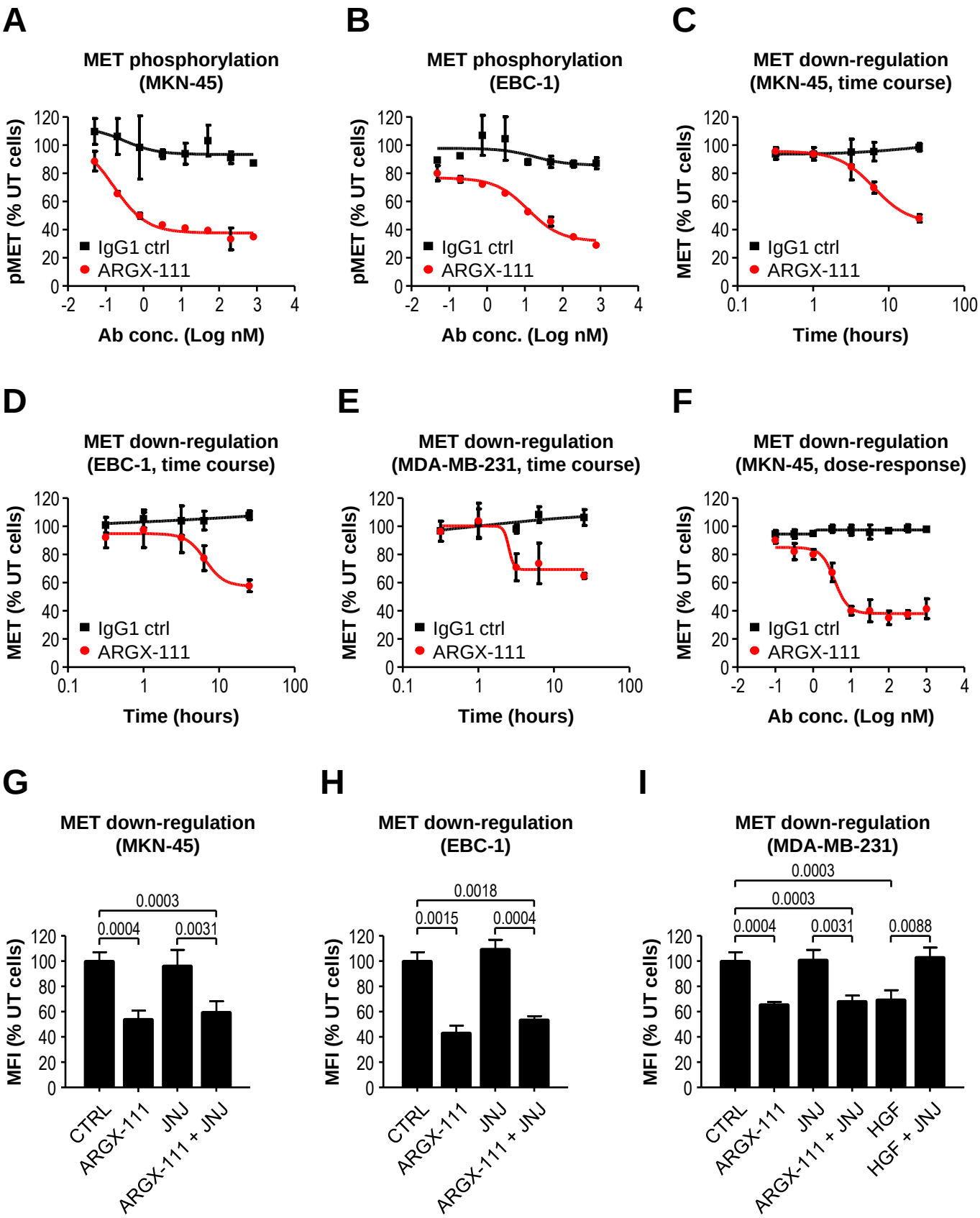
A
MET phosphorylation
(MKN-45)
pMET (% UT cells)
IgG1 ctrl
ARGX-111
Ab conc. (Log nM)
B
MET phosphorylation
(EBC-1)
pMET (% UT cells)
IgG1 ctrl
ARGX-111
Ab conc. (Log nM)
C
MET down-regulation
(MKN-45, time course)
MET (% UT cells)
IgG1 ctrl
ARGX-111
Time (hours)
D
MET down-regulation
(EBC-1, time course)
MET (% UT cells)
IgG1 ctrl
ARGX-111
Time (hours)
E
MET down-regulation
(MDA-MB-231, time course)
MET (% UT cells)
IgG1 ctrl
ARGX-111
Time (hours)
F
MET down-regulation
(MKN-45, dose-response)
MET (% UT cells)
IgG1 ctrl
ARGX-111
Ab conc. (Log nM)
G
MET down-regulation
(MKN-45)
MFI (% UT cells)
0.0003
0.0004
0.0031
CTRL
ARGX-111
JNJ
ARGX-111 + JNJ
H
MET down-regulation
(EBC-1)
MFI (% UT cells)
0.0018
0.0015
0.0004
CTRL
ARGX-111
JNJ
ARGX-111 + JNJ
I
MET down-regulation
(MDA-MB-231)
MFI (% UT cells)
0.0003
0.0003
0.0004
0.0031
0.0088
CTRL
ARGX-111
JNJ
ARGX-111 + JNJ
HGF
HGF + JNJ

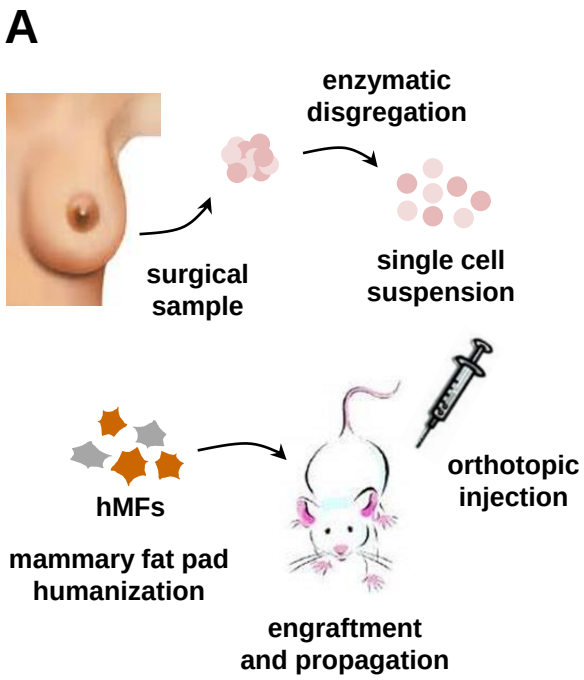
A
enzymatic
disgregation
surgical
sample
single cell
suspension
hMFs
mammary fat pad
humanization
orthotopic
injection
engraftment
and propagation

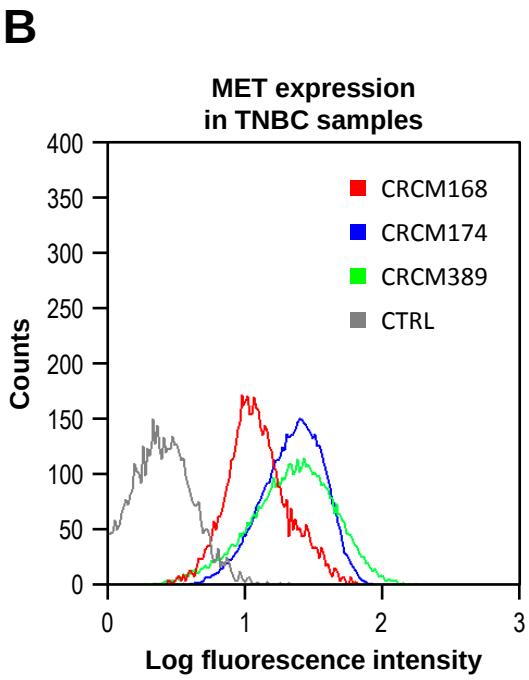
B
MET expression
in TNBC samples
CRCM168
CRCM174
CRCM389
CTRL
Counts
400
350
300
250
200
150
100
50
0
0
1
2
3
Log fluorescence intensity

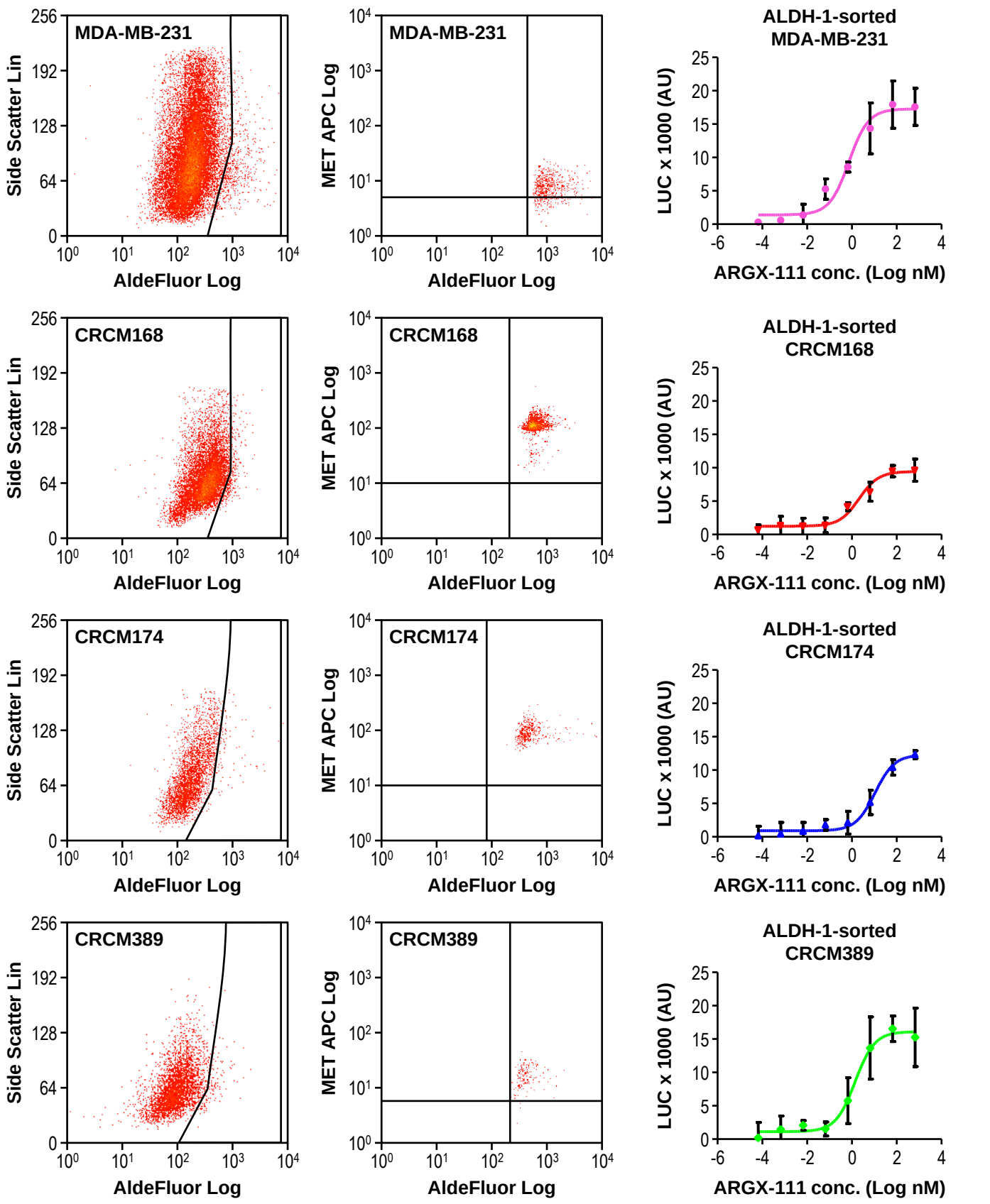
A
B
MDA-MB-231
CRCM168
CRCM174
CRCM389
Side Scatter Lin
AldeFluor Log
MET APC Log
ALDH-1-sorted
LUC x 1000 (AU)
ARGX-111 conc. (Log nM)